



# مجلة جامعة حجة

مجلة علمية محكمة - نصف سنوية - تصدرها جامعة حجة - العدد الثالث - (يونيو - ديسمبر) ٢٠٢٢م

الإمتصاص الضوئي لبلورة تنجستات الرصاص النقية

أ. عبدالرحمن الطواف

د. عبدالعزيز الزغبى

الفكر الاسلامي بين الأصالة والتجديد لنوازله

دراسة تحليلية تقويمية.

د. عبدالعزیز علي مفتن الورقي

رؤية مقترحة لإدارة الأزمات أثناء الحرب من وجهة نظر الأكاديميين والإداريين

بكليات المجتمع الخاصة بالجمهورية اليمنية

د. محمد قاسم قحوان

د. أمة الله دحان المسهلي

أثر الحرب على احتياجات الشباب الجامعي بالجمهورية اليمنية

د. منصور ناصر صالح جبارة

Evidence of Mixed Ionic-Electronic Conduction in

Double Perovskites Series  $x\text{MnxTiO}_6\text{-SrLaFe1}$ :

Structural and Dielectric Impedance Studies

د. يوسف الصباح



# Hajjah University Journal

A Reffered Bi-annual Journal issued by Hajjah University - Issue no (3) - (June-December) 2022

Optical Absorption of Pure Lead Tungstate Crystal

Abdulrahman Altawwaf

Dr. Abdulaziz Alzughbi

Islamic Thought Between Originality and Renewal of its Adversities:  
An Analytical Evaluative Study

Dr. Abdulaziz Ali Muften Al-Waraq

A Proposed Vision for Crisis Management during War from  
Academics & Administrators' Perceptive in  
Private Community Colleges in the Republic of Yemen

Dr. Muhammad Qasem Qahwan

Dr. Amatullah Dahan Al-Mes'hali

Impact of War on University Youth in the Republic of Yemen

Dr. Mansour Nasser Saleh Jobara

Evidence of Mixed Ionic-Electronic Conduction in  
 $\text{SrLaFe}_{1-x}\text{MnxTiO}_6$  Double Perovskites Series:  
Structural and Dielectric Impedance Studies

Dr. Yousef A. Alsabah



جامعة حجة  
HAJJAH UNIVERSITY

مجلة جامعة حجة للعلوم الإنسانية والتطبيقية  
مجلة علمية محكمة نصف سنوية تصدرها جامعة حجة  
العدد الثالث ( يوليو – ديسمبر 2022 )

الهيئة الاستشارية

- أ. د . علي يحيى شرف الدين  
أ. د . حمود ناصر نصار  
أ.د. يحيى يحيى العلي  
أ.د . عبدالعزيز هادي العامري  
أ. د . حسن ناصر سرار  
أ. د . محمد عبدالله حميد  
أ. د . محمد شوعي دموم  
أ. د . بشرى علي العماد  
أ. د . هادي عبدالله شمسان  
أ. د . صالح علي النهاري  
أ.د. سلام عبود حسن

الهيئة الاشرافية  
و هيئة التحرير

الإشراف العام

أ.د. محمد عدالوهاب الخالد  
رئيس الجامعة

رئيس التحرير

أ. د . عبده محمد سحلول

مدير التحرير

د . حمير يحيى محمد الأعور

نائب مدير التحرير

أ.د . محمد شوقي ناصر الأعور

هيئة التحرير

د. أمة الله دحان المسهلي

د. محمد علي القبلي

د. عبدالعزيز علي الورقي

د. إبراهيم أحمد الحمزي

د. بشرى ناصر المصوبع

د. عبدالغني حميد محيي

د. علي أحمد الهلاني

د. مطهر أحمد حميد

د. نبيل محمد مجلي

د. عادل يحيى الجبري

د. حسين أحمد راجحي

د. يوسف أحمد الصباح

المراجع اللغوي ( لغة انجليزية)

د. رضوان الشارف

مجلة علمية محكمة تصدرها جامعة حجة وتهتم بنشر لأبحاث العلمية المحكمة في العلوم  
الإنسانية والتطبيقية باللغتين العربية والانجليزية



جامعة حجة  
HAJJAH UNIVERSITY





جامعة حجة  
HAJJAH UNIVERSITY

**ضوابط وإجراءات قبول النشر في المجلة:**

هناك ضوابط وإجراءات لا بد من إتباعها عند تقديم البحوث للنشر في المجلة العلمية لجامعة حجة وهي:

**أولاً: الضوابط العامة لقبول النشر في المجلة:**

1 - المجلة تقبل جميع البحوث باللغتين العربية والإنجليزية، التي يجب أن تتوفر فيها الشروط الآتية:  
أ - أن يكون البحث المقدم أصيلاً ويعالج قضية معينة بذاتها، وتتوافر فيه الشروط العامة للبحث العلمي المعتمد على القواعد العلمية والمنهجية المتعارف عليها في كتابة البحوث الأكاديمية، في مختلف المجالات الإنسانية والتطبيقية.

ب - أن يكون البحث مكتوباً بلغة سليمة وواضحة سواء في العربية أو في الإنجليزية، وأن يكون مصححاً لغوياً ومطبعياً.

ج - أن يحزر البحث باللغة العربية بخط: Traditional Arabic حجم (14)، وبالنسبة للبحوث باللغة الإنجليزية بخط (Times New Roman) والحجم (12)، أما العناوين فينفس الخط لكن بخط عريض، وألا تزيد صفحات البحث عن (30) صفحة متضمنة المصادر والمراجع.

د - يجب أن تكون الجداول والرسوم والأشكال في مواضعها الصحيحة، وأن تكون شاملة للعناوين والبيانات الضرورية، وألا تتجاوز أبعاد الرسوم والأشكال والجداول حجم صفحة الطباعة.

هـ - هوامش إعداد الصفحة تكون: 3 سم على اليمين، و2 سم في باقي الجهات: العلوي، الأيسر، الأسفل.

و- أن يكون البحث ملتزماً بدقة التوثيق، ويتبع في توثيق المصادر والمراجع أسلوب (APA) الإصدار السادس. وفيما يتعلق بقائمة المراجع:

- ضرورة التحقق من تطابق المراجع التي ذكرت في المتن وتلك التي في قائمة المراجع.
- ترتيب المراجع هجائياً (أ، ب، ت، ث..) في قائمة واحدة حسب الاسم الأخير للمؤلف، ولا تصنف حسب نوعها (كتب، مجلات، مذكرات..).
- إهمال (ال) التعريف عند الترتيب الهجائي للمراجع باللغة العربية.
- ترتيب قائمة المراجع دون ترقيم متسلسل.
- يتم التوثيق في المتن بذكر الاسم الأخير لصاحب المرجع وسنة النشر ورقم الصفحة كالتالي: (الهمداني، 2018، ص 22)، أو في أسفل الصفحة حسب طبيعة البحث.
- ترتيب قائمة المراجع العربية أولاً، ثم الإنجليزية، ثانياً على الشكل الآتي:

**أولاً المصادر:**

اللقب، الاسم كاملاً.(سنة النشر). عنوان المصدر بخط مائل، اسم المحقق أو المترجم(إن وجد)، (رقم الطبعة إن وجد ويرمز للطبعة بالحرف ط)، مكان النشر: الناشر.  
ثانياً: المراجع:

• **توثيق الكتب:**

اللقب، الاسم كاملاً.(سنة النشر). عنوان الكتاب بخط مائل،(رقم الطبعة إن وجد ويرمز للطبعة بالحرف ط)، مكان النشر: الناشر.

• **توثيق الدوريات والمجلات العلمية:**

اللقب، الاسم كاملاً.(سنة النشر). عنوان البحث أو المقال، اسم المجلة بخط مائل، رقم المجلد إن وجد (رقم العدد)، الصفحات التي ورد فيها البحث.

• **توثيق الموسوعات العلمية:**

اللقب، الاسم كاملاً.(سنة النشر). عنوان المقال، اسم الموسوعة بخط مائل،(ج. رقم الجزء، ص. مدى الصفحات)، مكان النشر: الناشر.

• **توثيق المؤتمرات والندوات:**

اللقب، الاسم كاملاً.(تاريخ الإنعقاد). عنوان البحث أو الورقة العلمية بخط مائل، اسم المؤتمر أو الندوة، مكان وبلد الانعقاد.

• **توثيق أطروحات الماجستير والدكتوراه:**

اللقب، الاسم كاملاً.(سنة المناقشة). عنوان الرسالة بخط مائل، نوعها، اسم الجامعة، بلد النشر.  
• توثيق مقالات الإنترنت:

اللقب، الاسم كاملاً.(سنة نشر المقال، اليوم، الشهر). عنوان المقال بخط مائل، تم استرجاعها في تاريخ: اليوم والشهر والسنة، عنوان الموقع الإلكتروني.

2- يشترط ألا يكون البحث قد نشر من قبل، أو مقدم للنشر في أي مجلة أخرى، ويقدم إقرار بذلك.

3- من حق المجلة إخراج البحث وإبراز عناوينه بما يتناسب مع أسلوبها في النشر.

4- ترحب المجلة بنشر ما يأتي إليها من ملخصات الرسائل الجامعية التي نوقشت وتم إجازتها في كافة مجالات العلوم الإنسانية والتطبيقية، شريطة أن يكون ملخص الرسائل من أصحاب الرسائل أنفسهم.

5-تحديد نسبة الاقتباس في البحوث عبر استخدام برنامج (Plagiarism) ب (20%) للأقسام العلمية، و(40%) للأقسام الأدبية.

## ثانياً: إجراءات النشر بالمجلة:

- 1 - ترسل البحوث والمراسلات إلى جامعة حجة على العنوان التالي:  
الجمهورية اليمنية - محافظة حجة - ص . ب ( ..... ) مجلة جامعة حجة  
هاتف: (009677224074) تليفاكس (009677224074) البريد الإلكتروني: (.....)
  - 2-يسلم البحث المقدم للنشر من أصل وثلاث نسخ ورقية مطبوعة على ورق (A4)، ونسخة إلكترونية (Word) و(PDF) ومحفوظة بقرص مدمج (CD)، ويشترط أن تكون المادة مطبوعة بمسافة 1.25(واحد وربع) وذلك إلى عنوان المجلة أعلاه، أو على البريد الإلكتروني، بحيث يظهر في غلاف البحث اسم الباحث ولقبه العلمي، ومكان عمله، ومجال تخصصه وإيميله.
  - 3 - يرفق بالبحث ملخصان باللغتين العربية والإنجليزية على ألا يزيد عدد كلمات كل ملخص منها عن (200) كلمة.
  - 4-يرفق الباحث نسخة مختصرة عن سيرته الذاتية، متضمنة اسم الباحث وعنوانه، وأرقام هواتفه لكي يسهل التواصل معه عند الضرورة.
  - 5- في حالة قبول البحث مبدئياً، يتم إحالته إلى محكمين من ذوي الخبرة والاختصاص في مجال البحث، ويتم اختيارهم بسرية تامة، ولا يعرض عليهم اسم الباحث أو بياناته، وذلك لإبداء آرائهم حول مدى أصالة البحث، وقيمتها العلمية، ومدى التزام الباحث بالمنهجية المتعارف عليها، ويطلب من المحكم تحديد مدى صلاحية البحث للنشر في المجلة من عدمه.
  - 6- يخطر الباحث بقرار صلاحية بحثه للنشر من عدمه خلال شهر على الأكثر من تاريخ تسليمه للبحث.
  - 7- في حالة ورود ملاحظات من المحكمين، ترسل تلك الملاحظات إلى الباحث بهدف إجراء التعديلات اللازمة، على أن تعاد للمجلة في مدة أقصاها أسبوعين.
  - 8- يمنح صاحب البحث المنشور نسخة ورقية واحدة من عدد المجلة مع ثلاث مستلآت من بحثه.
  - 9- نظراً لتنوع الدراسات والبحوث الإنسانية والتطبيقية، فإنه يتم التعامل وفق نمط عام لعناصر التحرير، بحيث:
- أ- تحرر البحوث النظرية بحيث تتضمن: مقدمة تحتوي على عناصر الموضوع، والمشكلة، العرض (يحتوي التفرع المنهجي: عناصر رئيسية وعناصر فرعية، مرتبة ترتيباً تصاعدياً)، خاتمة تتضمن نتائج البحث (وليس تلخيصاً للبحث)، قائمة بمصادر ومراجع البحث منظمة ومرتبطة وفق النظام المعمول به في هذه المجلة.
- ب- أما البحوث والدراسات الميدانية فيجب أن تتضمن: المقدمة، المشكلة، أهداف الدراسة، أهمية

الدراسة، حدود الدراسة، تحديد مصطلحات الدراسة، الإطار النظري، الدراسات السابقة، إجراءات الدراسة الميدانية، وتتضمن منهج الدراسة، مجتمع وعينة الدراسة، أدوات الدراسة، إجراءات التطبيق، الأساليب الإحصائية، عرض نتائج الدراسة ومناقشتها، التوصيات والمقترحات، قائمة المراجع.

### ثالثاً: رسوم التحكيم والنشر في المجلة:

تحدد المجلة مقابل نشر البحوث والتحكيم الرسوم التالية:

- البحوث المرسلة من داخل الجمهورية اليمنية ( 20000 ) عشرون ألف ريال يمني.
- منتسبو جامعة حجة (10000) عشرة ألف ريال يمني.
- البحوث المرسلة من خارج الجمهورية اليمنية ( 150 \$ ) مائة وخمسون دولار أمريكي .
- هذه الرسوم غير قابلة للإرجاع سواء تم قبول البحث للنشر أم لم يتم النشر .

### أحكام عامة: (جميع حقوق الطبع محفوظة للمجلة)

- 1- البحوث المنشورة في المجلة لا تعبر بالضرورة عن توجه الجامعة وإنما تعبر عن آراء أصحابها.
- 2- تؤول جميع حقوق النشر للمجلة، ولا يجوز نشر جزء من المجلة أو اقتباسه دون الحصول على موافقة خطية من رئيس هيئة تحرير المجلة.
- 3- الأبحاث التي لم تتم الموافقة على نشرها لا تعاد إلى الباحثين .

البحوث المنشورة في المجلة لا تعبر بالضرورة عن توجه الجامعة وإنما تعبر عن آراء أصحابها

(رقم الإيداع (507) (7 / 11 / 2021 م) (الهيئة العامة للكتاب والنشر والتوزيع - دار الكتب- صنعاء)  
( جميع حقوق الطبع محفوظة للمجلة )

الحمد لله الذي علم بالقلم علم الإنسان ما لم يعلم، والصلاة والسلام على معلم البشرية وهاديها سيدنا محمد وعلى آله الطيبين الطاهرين، ورضي الله عن الصحابة أجمعين، ومن تبعهم بإحسان إلى يوم الدين، وبعد: يسرنا في هذه الاطلالة ومع صدور العدد الثاني من المجلة العلمية المحكمة بجامعة حجة أن نتقدم بخالص الشكر والثناء إلى رئيس جامعة حجة الأستاذ الدكتور/ محمد عبدالوهاب الخالد، المشرف العام للمجلة، وإلى الهيئة الإدارية للمجلة، وهيئة التحرير المجلة والهيئة الاستشارية، وفي مقدمتهم مدير تحرير المجلة، الدكتور/ حمير يحيى الأعور، ونائب مدير التحرير الأستاذ الدكتور/ محمد شوقي الأعور على الجهود التي بذلوا وما زالوا لتستمر هذه المجلة في الصدور. حيث يتزامن صدور هذا العدد الثاني من المجلة مع استمرار الحراك الأكاديمي النشط بجامعة حجة، والبدء في افتتاح عدد من الكليات والبرامج الأكاديمية الجديدة بالجامعة ومنها: كلية الطب والعلوم الصحية، وكلية الزراعة والطب البيطري بعبس، وكلية الشريعة والقانون، وإضافة العديد من البرامج الجديدة بالدراسات العليا (ماجستير)، بالأقسام الآتية: قسم اللغة العربية، وقسم علوم الحياة، وقسم علوم القرآن، وقسم الدراسات الإسلامية، وقسم التاريخ، إضافة إلى العمل على أتمتة عمل كافة الكليات والإدارات بالجامعة، وتحديث الموقع الالكتروني للجامعة الذي يعد النافذة التي تطل منها الجامعة على العالم الخارجي، ويطل العالم الخارجي من خلالها على جامعة حجة ليتعرف على بنية الجامعة وبرامجها الأكاديمية وأنشطتها العلمية والثقافية وغيرها، ومنسبها من الأكاديميين والإداريين والطلاب، كما تعمل الجامعة بخطى حثيثة ومدروسة على تطوير بنيتها، وتحديث برامجها الأكاديمية وفق معايير الجودة والاعتماد الأكاديمي سعياً منها - كما هو شأن كافة الجامعات اليمنية - إلى الحصول على الاعتماد الأكاديمي.

وتشجيعاً للباحثين من الأكاديميين دعمت رئاسة الجامعة هذين العديدين، وأعطت فرصة للباحثين لنشر أبحاثهم في هذه المجلة (مجاناً)، وبهذه المناسبة ومن خلال هذا المنبر العلمي أَدْعُو كافة الأكاديميين والباحثين، سواء في جامعة حجة أم في غيرها من الجامعات اليمنية، والإقليمية، والعربية إلى إرسال أبحاثهم على عنوان المجلة التي تتشرف باستقبال ونشر الأبحاث سواء في العلوم الإنسانية، أو العلوم التطبيقية.

سائلين الله تعالى التوفيق للجميع

رئيس التحرير

أ.د/ عبده محمد سحلول



جامعة حجة  
HAJJAH UNIVERSITY

## المحتويات

الصفحة	الباحث	الوضوع	م
13 3-0	أ. عبدالرحمن الطواف باحث دكتوراه - قسم الفيزياء - كلية التربية - جامعة حجة د. عبدالعزيز الزغبى قسم الفيزياء - كلية العلوم - جامعة دمشق - سوريا	الإمتصاص الضوئي لبلورة تنجستات الرصاص النقية	1
31 - 64	د . عبدالعزيز علي مفتن الورقي أستاذ العقيدة والفكر الاسلامي المساعد بكلية التربية - جامعة حجة رئيس قسم علوم القرآن	الفكر الاسلامي بين الأصالة والتجديد لنوازله دراسة تحليلية تقييمية.	2
65 - 106	د . محمد قاسم قحوان أستاذ أصول التربية المشارك - جامعة عمران د . أمة الله دحان المسهلي أستاذ أصول التربية المساعد - جامعة حجة	رؤية مقترحة لإدارة الأزمات أثناء الحرب من وجهة نظر الأكاديميين والإداريين بكليات المجتمع الخاصة بالجمهورية اليمنية	3
107 - 250	د . منصور ناصر صالح جُبارة أستاذ علم النفس التربوي المساعد ورئيس قسم العلوم التربوية والنفسية - كلية التربية - جامعة صعدة	أثر الحرب على احتياجات الشباب الجامعي بالجمهورية اليمنية	4
1 - 29	Dr. Yousef A. Alsabah Department of Physics, Faculty of Education and Applied Science, Hajjah University, Hajjah, Yemen	Evidence of Mixed Ionic- Electronic Conduction in SrLaFe <sub>1-x</sub> MnxTiO <sub>6</sub> Double Perovskites Series: Structural and Dielectric Impedance Studies	5



جامعة حجة  
HAJJAH UNIVERSITY

**Evidence of Mixed Ionic-Electronic Conduction in SrLaFe<sub>1-x</sub>Mn<sub>x</sub>TiO<sub>6-δ</sub> Double  
Perovskites Series: Structural and Dielectric Impedance Studies.**

Dr.Yousef A. Alsabah

**Department of Physics, Faculty of Education and Applied Science, Hajjah  
University, Hajjah, Yemen****Abstract**

The structural and the electrical properties of the double perovskite compounds SrLaFe<sub>1-x</sub>Mn<sub>x</sub>TiO<sub>6-δ</sub>, (x= 0, 0.33, 0.67 & 1.0) were studied via X-ray diffraction (XRD) and the dielectric impedance measurements. The preparation of the compounds was successfully achieved through the precursor solid state reaction in the air at 1250 °C. The purity phase and the crystal structures of the compounds were determined by means of the standard Rietveld refinement method using the FullProf suite. The best fitting results showed that SrLaFeTiO<sub>6-δ</sub> was orthorhombic with space group Pnma, both SrLaFe<sub>0.67</sub>Mn<sub>0.33</sub>TiO<sub>6-δ</sub> and SrLaFe<sub>0.33</sub>Mn<sub>0.67</sub>TiO<sub>6-δ</sub> was a cubic structure with space group Fm3m while SrLaMnTiO<sub>6-δ</sub> was tetragonal with I/4m space group. The charge density maps obtained for these structures indicated that the compounds show an ionic and mixed ionic–electronic conduction. The dielectric impedance measurements were carried out in the range of 20 Hz to 1MHz and their analysis showed that there are more than one relaxation mechanisms of Debye type. Doping with Mn was found to reduce the dielectric impedance of the samples and the major contribution to the dielectric impedance was established to change from a capacitive in case of SrLaFeTiO<sub>6-δ</sub> to a resistive in SrLaMnTiO<sub>6-δ</sub>. The fall in the values of the electrical resistance maybe related to the possible occurrence of the double exchange (DEX) mechanism among the Mn ions providing that there is oxygen deficiency in the samples. DC-resistivity measurements were revealed that SrLaFeTiO<sub>6-δ</sub> was an insulator while SrLaMnTiO<sub>6-δ</sub> was showing semiconductor–metallic transition at ~ 250 K which in support of the DEX interaction. The dielectric impedance of SrLaFe<sub>0.67</sub>Mn<sub>0.33</sub>TiO<sub>6-δ</sub> was found to be similar to that of (La,Sr)(Co,Fe)O<sub>3-δ</sub>, the mixed ionic–electronic conductor (MIEC) model. The occurrence of a mixed ionic–electronic state in these

المخلص

5

## **Evidence of Mixed Ionic-Electronic Conduction in SrLaFe<sub>1-x</sub>Mn<sub>x</sub>TiO<sub>6</sub> Double Perovskites Series: Structural and Dielectric Impedance Studies**

Yousef A. Alsabah<sup>1\*</sup>

Department of Physics, Faculty of Education and Applied Science, Hajjah University, Hajjah, Yemen

\* Correspondence author email: [y.a.alsabah@gmail.com](mailto:y.a.alsabah@gmail.com)

### **المخلص**

دورست الخصائص البنيوية والكهربائية لمركبات البيروفسكايت الثنائية  $SrLaFe_{1-x}Mn_xTiO_{6-\delta}$ , ( $x = 0, 0.33, 1.0$ ) باستخدام تقنية حيود الأشعة السينية (XRD) وقياسات مقاومة العزل الكهربائي. حُضرت المركبات بنجاح من خلال تفاعل الحالة الصلبة للمواد الأولية في الهواء عند 1250 درجة مئوية. دُرست درجة النقاء للعينات المحضرة والتراكيب البلورية للمركبات بطريق طريقة رينفولد وباستخدام برنامج الفل بروف. ظهرت أفضل النتائج الملائمة أن  $SrLaFeTiO_{6-\delta}$  كان معيني مع مجموعة الفراغ  $Pnma$ ، بينما أخذت كلا العينتين  $SrLaFe_{0.67}Mn_{0.33}TiO_{6-\delta}$  and  $SrLaFe_{0.33}Mn_{0.67}TiO_{6-\delta}$  هيكلًا مكعبًا مع مجموعة فراغية  $Fm3m$ ، بينما أظهرت العينة  $SrLaMnTiO_{6-\delta}$  الشكل الأحادي الميل مجموعة الفراغ  $I4/m$ . أشارت خرائط كثافة الشحنة لهذه التراكيب إلى أن المركبات تظهر توصيلاً أيونيًا ومختلطاً أيونيًا إلكترونيًا. تم إجراء قياسات مقاومة العزل الكهربائي في نطاق 20 هرتز إلى 1 ميجا هرتز وأظهر تحليلها أن هناك أكثر من آلية استرخاء من نوع ديبياي. كما وجد ان زيادة التطعيم بالمنجنيز تسبب في إنقاص ثابت العزل الكهربائي للعينات وكما ان المتسبب الرئيسي في قيم ثابت العزل الكهربائي ناتج للتغيير من السعة الكهربائية في حالة  $SrLaFeTiO_{6-\delta}$  وإلى المقاومة الكهربائية في  $SrLaMnTiO_{6-\delta}$  كما ان الانخفاض في قيم المقاومة الكهربائية مرتبطاً باحتمال حدوث آلية التبادل المزدوج (DEX) بين أيونات المنجنيز بشرط وجود نقص الأكسجين في العينات. تم الكشف عن قياسات المقاومة DC أن العينة  $SrLaFeTiO_{6-\delta}$  مادة عازلة بينما أظهرت العينة  $SrLaMnTiO_{6-\delta}$  انتقالاً إلى شبه موصل معدني عند حوالي 250 كلفن. تم العثور على المعاوقة الكهربائية للمركب  $SrLaFe_{0.67}Mn_{0.33}TiO_{6-\delta}$  لتكون مماثلة لتلك الخاصة للمركبات  $(La,Sr)(Co,Fe)O_{3-\delta}$ ، الموصل الأيوني الإلكتروني المختلط (MIEC). ان الحالة الإلكترونية الأيونية المختلطة تؤهل هذه المركبات لاستخدامها كأقطاب موجبة في خلايا وقود الأكسيد الصلب (SOFC).

**Key words:** Impedance spectroscopy; mixed ionic-electronic conductor (MIEC); Perovskite oxide; solid oxide fuel cells (SOFC)

## 1. Introduction

The solid oxide fuel cells (SOFC) are receiving great attention from many research groups for their promising applications as a relatively clean and cheap source of energy[1-3]. The utilization of the SOFC is faced by many difficulties that are to be solved. A major one is a coke onto the surface of the Ni-Yttrium stabilized zirconia (Ni-YSZ) anode of the SOFC. The NiO acts as catalysis and reacts with the methane (CH<sub>4</sub>) fuel which splits into carbon and hydrogen[4-5] and causing deposition of carbon on the anode surface. New stable anode materials were developed in order to solve this problem.

The mixed ionic-electronic conductor (MIEC) material is preferred to replace the Ni-YSZ anode. Such a property is found in numerous perovskites structures such as (La<sub>0.5</sub>Sr<sub>0.5</sub>)<sub>1-x</sub>Fe<sub>1-y</sub>Al<sub>y</sub>O<sub>3- $\delta$</sub>  (x=0-0.05; y=0-0.3)[6], SrSn<sub>1-x</sub>Fe<sub>x</sub>O<sub>3-x/2+ $\delta$</sub>  [7] and (La,Sr)(Fe,Ni)O<sub>3</sub> [8]. Not only the presence of MIEC is important; but also the values of the ionic ( $\sigma_e$ ) and the electronic ( $\sigma_i$ ) conductivities. For a perovskite to be qualified as an efficient electrode and current collector, the conditions  $\sigma_i \geq 0.1$  S/cm and  $\sigma_e \geq 100$  S/cm[9] were fulfilled, so as to be an alternative for the Ni-YSZ anode.

The perovskites structures are considered to be stable under electrochemical reactions. P. Zhang et al [4] have reported that a double perovskite SOFC anode based on Sr<sub>2</sub>CoMoO<sub>6</sub> is assumed to be a good MIEC where it gave a maximum power density of 1017mW/cm<sup>2</sup> when La<sub>0.8</sub>Sr<sub>0.12</sub>Ga<sub>0.83</sub>Mg<sub>0.17</sub>O<sub>2.815</sub> is used as a solid electrolyte. To qualify a double perovskites material as a good SOFC anode, some fundamental properties were investigated beforehand. The dielectric impedance is one of the sensitive tools to inspect the relaxation

mechanism and conductivity of the SOFC materials[9-12] as well as to probe the effect of the hydrogen on the electrical conductivity[8] usually encountered in the operation of the SOFC. It is also used to probe the mixed ionic-electronic conductivity of materials[13]. T. Xia et al[14] had studied the dielectric and the conductivity of Sr<sub>2</sub>Fe<sub>1-x</sub>M<sub>x</sub>NbO<sub>6</sub> (M= Zn and Cu) under variable oxygen partial pressure. They found out that the conductivity of this material increases and it is chemically stable under oxygen partial pressure between 1 atm and 10<sup>-22</sup> atm at 873 K. The increase of the conductivity was related to the charge disproportionation reaction of the Fe<sup>3+</sup> ions. The dielectric impedance measurements carried out by Q. Liu et al on Sr<sub>2</sub>Fe<sub>1.5</sub>Mo<sub>0.5</sub>O<sub>6</sub> [3] revealed that it is sensitive to temperature and hydrogen. The conduction was explained in terms of the equilibrium reaction between Fe<sup>3+</sup> + Mo<sup>5+</sup> ↔ Fe<sup>2+</sup> + Mo<sup>6+</sup>. The dielectric impedance had also been done by D. Marrero-Lopez et al on Sr<sub>2</sub>MgMoO<sub>6-δ</sub> where the effect of H/Ar<sub>2</sub> mixture and the air have been investigated[15].

The iron-containing double perovskites have shown a variety of electrical conductivity. The Sr<sub>2</sub>FeMoO<sub>6</sub> is a half-metallic magnetic material that is useful in the spintronics application[16] while the Fe-rich Sr<sub>2</sub>Fe<sub>1.5</sub>Mo<sub>0.5</sub>O<sub>6</sub> is mixed-ionic electronic conductor[9]. The difference in the electrical conductivity of SrLaFeTiO<sub>6</sub> and SrLaMnTiO<sub>6</sub> may be related to the content and transport properties of the Fe and the Mn ions in both compounds.

In the present work, we study the doping effect of the Mn ions in the Fe-site of the double perovskites SrLaFeTiO<sub>6</sub> and investigate its suitability as MIEC conductors. The dielectric impedance measurements will be used to probe such property with the help of some equivalent circuit models proposed specifically for MIEC materials. In addition, the conductivity depends of SrLaFe<sub>1-x</sub>Mn<sub>x</sub>TiO<sub>6</sub>

( $x=0, 0.33, 0.67$  and  $1.0$ ) on the Mn concentration as the signature of possible MIEC materials will be investigated.

## 2. Experimental details

Polycrystalline samples are prepared from stoichiometric amounts of SrCO<sub>3</sub>, MnCO<sub>3</sub>, La<sub>2</sub>O<sub>3</sub>, MnO<sub>2</sub>, Fe<sub>2</sub>O<sub>3</sub> and TiO<sub>2</sub>. All materials are purchased from Alfa Acer and of purity not less than 99.9%. The Fe<sub>2</sub>O<sub>3</sub> and TiO<sub>2</sub> oxides are mixed and ground with a small amount of acetone for homogeneity and left to dry in air. The mixture is then heated at 900 °C for 12 hours. The obtained precursor is then mixed and heated with the prescribed stoichiometric amount of SrCO<sub>3</sub> and La<sub>2</sub>O<sub>3</sub> and then heated in a furnace at 900 °C for 12 hours. This process is repeated twice. The obtained powder was pressed into pellets under pressure of  $1.9 \times 10^8$  N/ m<sup>2</sup> for 30 seconds, and then heated at the same temperature for 24 hours with intermediate grindings. Finally, the samples are ground again and pressed before been sintered at 1200 °C for 24 hours at an ideal heating rate of 10 °C/min.

The X-ray diffraction is carried out using Bruker D8 Focus and Schimadzu 6000 diffractometers[17-18]. The data are collected in the angular  $2\theta$  range from 20° to 80° with step scan 0.01° and 3 sec/step using Cu- $k_{\alpha}$  radiation of wavelength  $\lambda = 0.1541$  nm. The collected data are then fed to the FullProf suite[19] in order to determine the lattice parameter, space group and atom positions.

Accurate dielectric impedance measurements are carried out on the samples which were in the form of pellets of about 1.24 cm diameter and 0.2 cm thickness. The two surfaces of each pellet are polished good and coated with a very thin layer of silver paste and checked for good conduction. The measurements are carefully taken at room temperature as a function of frequency in the range from 20 Hz to 1 MHz using a QuadTech LCR bridge model 1920 CE[20]. The LCR-bridge is interfaced to a PC and the data are

collected by in-lab written LabView program. The data are analyzed by the Easy analyzer program[21].

### **3. Results and discussion**

#### **3.1 The structural characterization and the charge density contour maps**

The XRD patterns measured at room temperature for the samples SrLaFeTiO<sub>6</sub>, SrLaFe<sub>0.67</sub>Mn<sub>0.33</sub>TiO<sub>6</sub>, SrLaFe<sub>0.33</sub>Mn<sub>0.67</sub>TiO<sub>6</sub> and SrLaMnTiO<sub>6</sub> are shown in Fig. 1. These patterns are subjected to careful analyses by means of the standard Rietveld methods employed in the FullProf suite. Three structural models are selected for the refinement processes for the accurate determination of the best crystal structure that matching the data. The double perovskite oxides can exist in one of the cubic, tetragonal or orthorhombic structures with the space group Fm3m, I/4m and Pnma respectively. The XRD characterization showed that prepared samples are of single-phase.

The results of the best fitting and the indexed peaks are also shown in Fig 1.. The quality of the proposed model was judged by means of the lowest value of the Bragg's reliability factors.

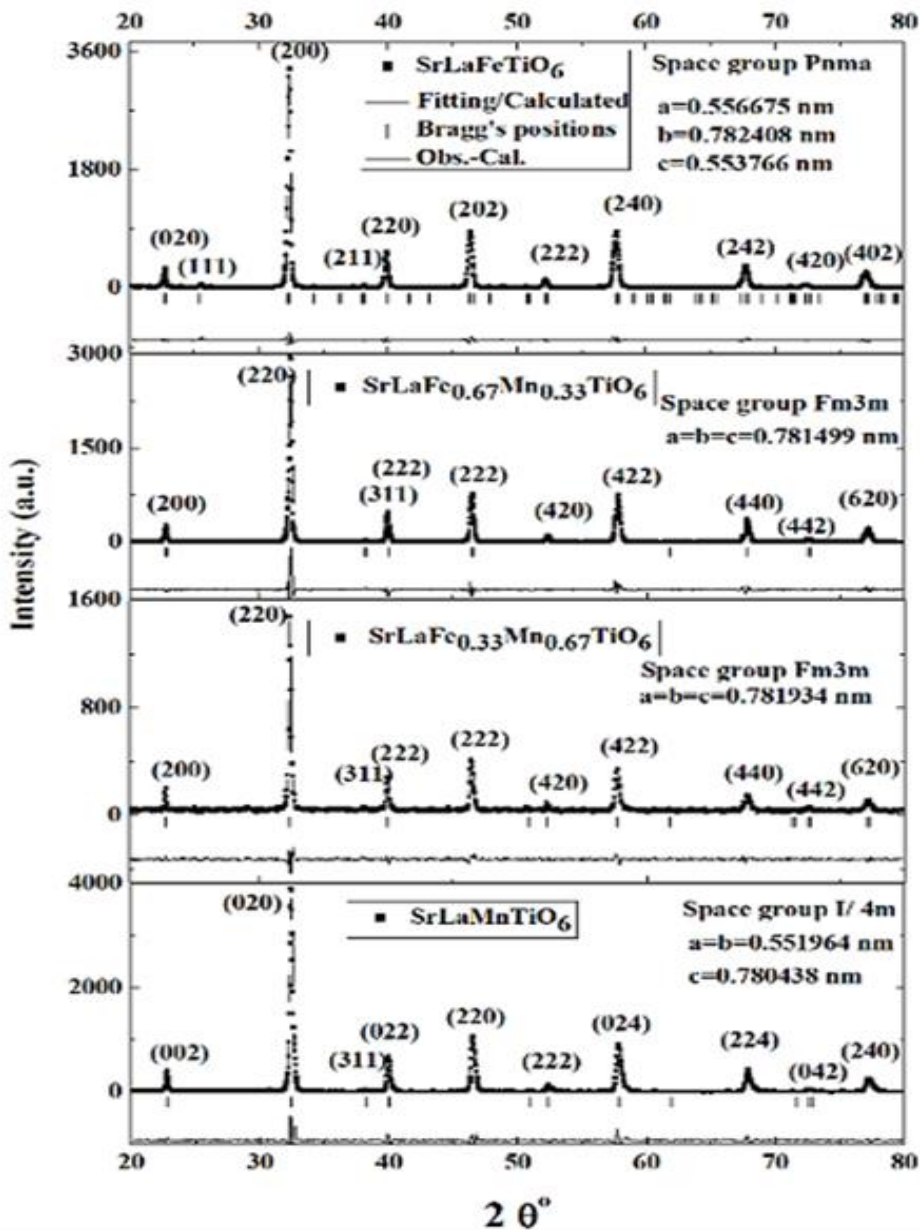


**Fig 1: The best fitting of the XRD patterns of prepared samples. The space group and the lattice parameters are shown.**

The XRD data and the results of the best fittings are fed to the GFourier program which is integrated into the FullProf suite. The GFourier (GF) is used to calculate the charge densities of the sample of interest. The results of the GF along the ab plane are shown in Fig 2. The effect of doping the Fe site by Mn is clearly seen in the contours maps of the charge densities of the present samples. Fig 2.a shows that SrLaFeTiO<sub>6</sub> is likely to be ionic conductor where no bonding between the Fe and Ti ions is observed. This behavior is disappeared in SrLaFe<sub>0.67</sub>Mn<sub>0.33</sub>TiO<sub>6</sub> (fig 2.b) and in SrLaFe<sub>0.67</sub>Mn<sub>0.33</sub>TiO<sub>6</sub> (fig 2.c) where a clear covalent bonding is detected. The mixed ionic-electronic state can be inferred from fig 2.d for SrLaMnTiO<sub>6</sub> where partial covalent bonding is observed. The degree of the competition between the ionic and the electronic conduction in these samples cannot be deduced accurately from the contours maps alone.

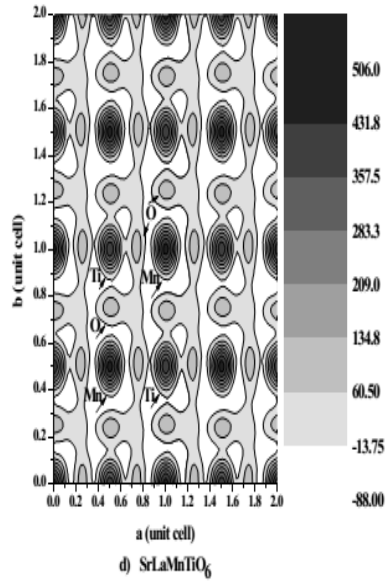
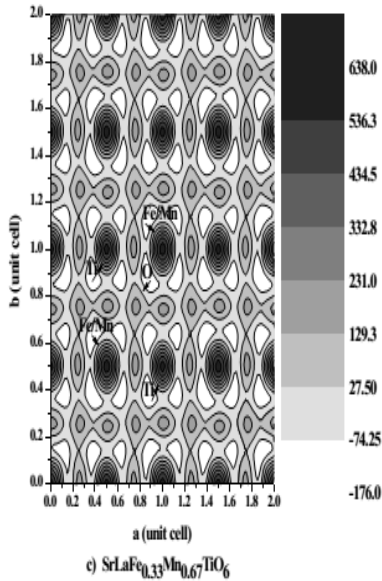
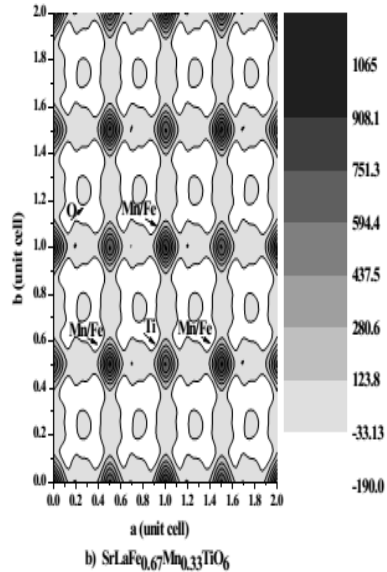
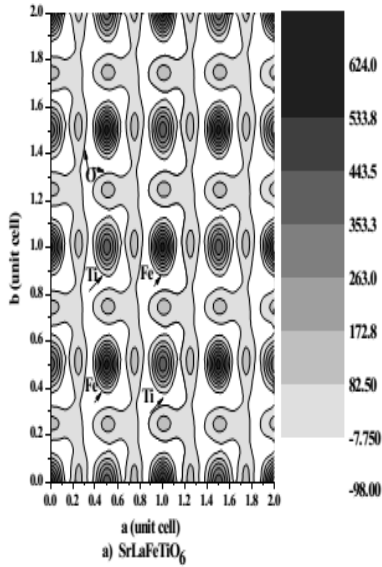


**Fig 2:**

**The contour maps in the ab-plane of each crystal system for prepared samples which obtained from the results of the best fitting of the XRD data.**

### **3.2 The frequency response of the dielectric impedance**

The Bode plots explicitly show the frequency dependence of the real and imaginary parts of impedance[22]. Careful inspection of the impedance response to the frequency in the form of Bode plots has a prime role in suggesting the equivalent circuit model fit the data and deducing the relaxation process (es) and other physical properties like MIEC[23]. Therefore, the results of the real ( $Z'$ ) and imaginary ( $Z''$ ) components of the impedance spectra which are measured in the frequency range from 20 Hz to 1MHz are firstly inspected in terms of the Bode plots.

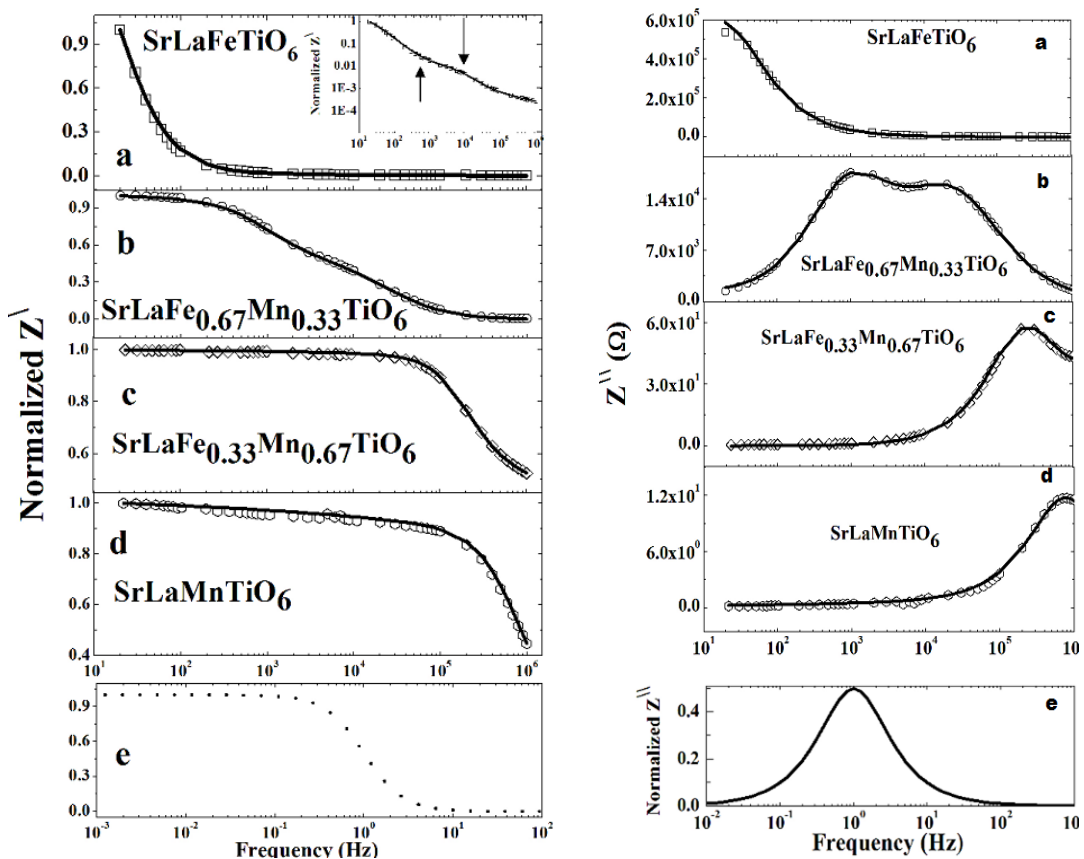


Fig 3: The Bode real dielectric impedance data measured for prepared samples. The lines represent the best fitting to the respective equivalent circuits. The data of the impedance are normalized in order to compare them with the simulated data shown in fig. 3.e.

The Bode plots for  $Z'$  and  $Z''$  as a function of frequency for the present samples are shown in figures 3 and 4, respectively. In fig. 3.a of SrLaFeTiO<sub>6</sub>, it can be observed that  $Z'$  is decreased as the applied frequency increased, while the opposite behavior is noticed in case of  $Z''$ . Moreover, changes in the slope are observed at around 300 Hz and at around 100 kHz, as indicated in the inset of fig 3.a. Such behavior indicates that there is more than a single relaxation mechanism in this sample.

Upon inclusion of the Mn ions in the Fe-site, the values of  $Z'$  for SrLaFe<sub>0.67</sub>Mn<sub>0.33</sub>TiO<sub>6</sub> (fig 3.b) appear varying slowly below 300 Hz, and then start decreasing with increasing the applied frequency. In SrLaFe<sub>0.33</sub>Mn<sub>0.67</sub>TiO<sub>6</sub> (fig 3.c) and SrLaMnTiO<sub>6</sub> (fig 3.d)  $Z'$  is found to be almost frequency independent up to about 82 kHz, and then is found to decrease as the frequency increases to 1 MHz.

The imaginary part of the impedance ( $Z''$ ) of SrLaFeTiO<sub>6</sub> (fig 4.a) is found to decrease as the applied frequency increases. For SrLaFe<sub>0.67</sub>Mn<sub>0.33</sub>TiO<sub>6</sub>, fig 4.b, two peaks ( $Z''_{max}$ ) are observed at around 1.37 kHz and 15.10 kHz in the plot of  $Z''$  which are indications of the occurrence of at least two relaxation times in the conduction process[24]. On the other hand,  $Z''$  shows peaks at around 243 kHz and 730 kHz for the samples SrLaFe<sub>0.33</sub>Mn<sub>0.67</sub>TiO<sub>6</sub> and SrLaMnTiO<sub>6</sub> as shown in fig 4.c and 4.d respectively. It is worthy to note here that the values of the frequency corresponds to the maximum  $Z''$  is found to increase with the content of the Mn atoms in the samples.

### 3.3 Equivalent circuits and modeling of the impedance data

In the figures 3.e and 4.e, simulations of the typical behavior of the Bode plots for the dielectric materials with a single relaxation time for an RC circuit are shown. These plots are generated assuming that  $Z' \propto \frac{1}{1+f^2}$  and  $Z'' \propto \frac{f}{1+f^2}$  where  $f$  is the frequency[25]. This circuit is simulated on a frequency span from  $10^{-3}$  up to  $10^6$  Hz. The range from  $10^{-2}$  up to  $10^3$  Hz is shown only in order to match the range of the frequency span of the measurement i.e. over 5 orders of magnitude. Below  $10^{-1}$  Hz, the response of the materials is found to be, almost, frequency independent; the contribution of the polarization resistance ( $R_p$ ) can be evaluated where it varies as  $\frac{1}{1+f^2}$ . When the frequency increases up to a few kHz it would decrease as  $\frac{f}{1+f^2}$  and then becomes frequency independent and then the resistance of the solid electrolyte ( $R_s$ ) can be evaluated. Further, from the imaginary part of the impedance, the relaxation frequency can be determined. By the help of this figure, the resistive and the capacitive contributions to the dielectric impedance can be inferred. The capacitive contribution leads to higher electrical resistance while the resistive contribution leads to low resistance[26].

Conventionally, to elucidate the conduction process (es) taking place in the dielectric materials, the Cole-Cole plots are generated and the data are fitted to

suitable equivalent circuits based on their analysis of the response of the dielectric impedance to the frequency. Generally, the Cole-Cole plots, i.e. the plots of  $Z'$  versus  $Z''$ , are used to inspect the contribution of the electrodes, the grain and the grain boundary effects to the dielectric impedance of materials[27]. In the ideal cases, these three contributions give rise to three arcs with three maxima that correspond to the relaxation frequency of an element of an equivalent circuit. These three arcs are usually modeled by a series combination of three sub-circuits each one is composed of a resistor connected in parallel with a capacitor (or a constant phase element (CPE)). The location of each arc is identified by the frequency where the arc of the grain boundary effect generally falls on a frequency span less than that of the grain effect. Therefore, the relaxation time of the grain boundary ( $\tau_{gb}$ ) effect is greater than that in the grain ( $\tau_b$ ) effect.

The  $Z'$  and  $Z''$  plots may appear as only part of an arc or as a single semicircle. The first situation indicates that the resistance of the grain boundary ( $R_{gb}$ ) could be very high compared to the resistance of the grain ( $R_g$ ), where the corresponding  $\tau_{gb}$  lies outside the frequency range of the measurements. Another case is for the typical insulating materials in which both  $R_g$  and  $R_{gb}$  are high. The semicircle shape may exist if  $R_g$  is small and the total resistance is dominated by  $R_{gb}$  and  $\tau_{gb}$  would be within the frequency range of the measurements[28-29].

By looking again into Bode plots shown in figures 3 and 4, and in combination with the expected response shown above, different features of the variation of  $Z'$  and  $Z''$  are noted with frequency in these samples. The compound

SrLaFeTiO<sub>6</sub> has shown a typical capacitive behavior as compared with fig 3.e, but the resistive contribution may be small and cannot simply be excluded. The effect of the Mn doping is found to change the major contribution to the dielectric impedance from a capacitive as observed in SrLaFeTiO<sub>6</sub> to a resistive one as in SrLaMnTiO<sub>6</sub>.

Strengthening of the resistive contribution is expected to lead to the presence of ionic and electronic conduction (MIEC). To look for MIEC, the data are to be modeled taking into consideration the capacitive and the resistive competition into the values of  $Z^{\prime}$  and  $Z^{\prime\prime}$  as shown in the Bode plots shown in fig 3 and fig 4 respectively. Modeling the MIEC state is discussed by many Authors [15-16]. F. S Baumann et al have studied the dielectric impedance of the well-defined (La,Sr)(Co,Fe)O<sub>3-δ</sub> model electrode[23] where the equivalent circuit model is based on J. Jamnik and J. Maier generalized equivalent circuit model for mixed conductors[30]. The response of the real and the imaginary parts of the impedance in the frequency range 0.1Hz to 1MHz and temperature 700 °C for (La,Sr)(Co,Fe)O<sub>3-δ</sub> is qualitatively similar to that of the sample SrLaFe<sub>0.67</sub>Mn<sub>0.33</sub>TiO<sub>6</sub>, but the Cole-Cole plots are found to be different. This difference may be related to the wide range of frequency used by Baumann et al. Thus, to model the impedance data of the present samples, which presented in the form of Cole-Cole plots, the equivalent circuit model of Baumann et al for MIEC materials is considered with slight modifications.

### 3.4 The complex Cole-Cole representation and the phase shift

The plot of  $Z''$  versus  $Z'$  for SrLaFeTiO<sub>6</sub> and the corresponding phase shift defined as  $\theta = \arctan(Z''/Z')$  are shown in fig 5.a and fig 6.b respectively. The Cole-Cole plot does not resemble a semicircle but a part of it with high values of  $Z'$  and  $Z''$ . Qualitatively, this means that the present sample did not show a semicircle may be because both the grain and the grain boundary resistances are high and the relaxation time lies outside the low-frequency limit. Quantitatively, the data are modeled using the equivalent circuit given in fig 7.a. This equivalent circuit is considered to deal with the effect of the electrode, grain boundary and grain size effects. The inclusion of the Warburg ( $W_s$ ) element is assumed to treat the diffusion in the transport process which is commonly observed in MIEC [31, 32]. The criterion for the best equivalent circuit is that it must fit simultaneously the data of  $Z'$  against frequency, the data of  $Z''$  against frequency, the Cole-Cole plot and the phase shift ( $\theta$ ) against frequency. This is because of some proposed equivalent circuits fit e.g. the Cole-Cole plot are failed in fitting the phase shift. This criterion is always looked and fulfilled in all the equivalent circuits proposed for prepared the samples. The lines in fig 5 represent the best fitting using the equivalent circuit shown in the fig 7.a and the fitting parameters are given in table 1.

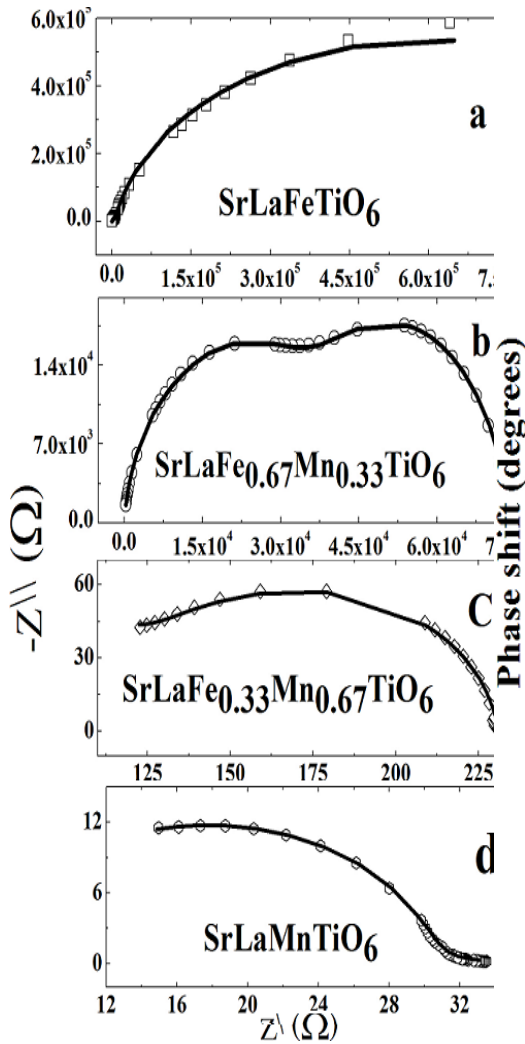


Fig 5: The complex Cole-Cole plots of prepared samples. The lines represent the best fitting to the respective equivalent circuits.

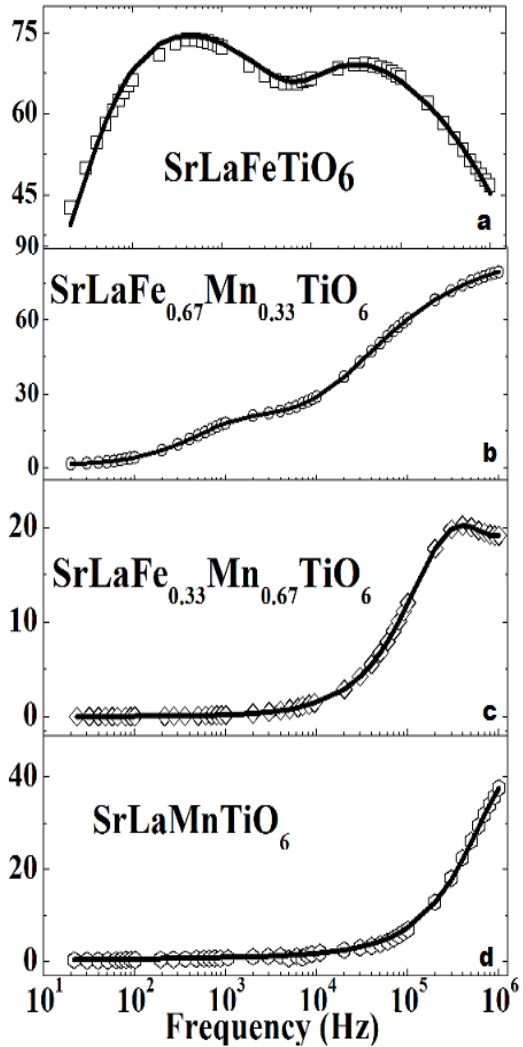


Fig 6: The phase angle shift calculated for prepared the samples. The lines represent the best fitting to the respective equivalent circuits.

The values of the grain and the grain boundary resistances are very high and the corresponding relaxation time ( $\tau = RC$ ) can be deduced if  $C$  is obtained[33]. The value of  $C$  is related to the impedance of the constant phase element (CPE) which is given by[33]

$$Z = \frac{1}{1 + p(i\omega)^n} \quad (1)$$

where  $p$  is a constant. The CPE element will represent a capacitor when the exponent  $n=1$  and  $p$  will equal  $C$ , the capacity of the capacitor. In the case when the value of  $n$  is less than 1, the capacitance can be given by

$$C = \frac{(p.R)^{1/n}}{R} \quad (2)$$

where  $R$  is the resistance connected in parallel with the concerned CPE element. The values of the  $C$  are calculated using equation 2 and the relaxation times are given in table 1. The calculated values of  $\tau_b$  and  $\tau_{gb}$  are found to be  $19.17 \times 10^{-6}$  sec and  $7.82 \times 10^{-3}$  sec respectively. The value of  $\tau_{gb}$  falls in the range of the relaxation time of the dipolar polarization mechanism while the value of  $\tau_b$  falls in the range of the hopping polarization mechanism. Further, the values of  $n$  of the CPE1 and CPE2 are large and equal to 0.95 and 0.92 respectively. This implies that the conduction is affected by the capacitive behavior of the grain boundary as inferred from the Bode plot of this sample. It cannot simply one say

that it is a purely ionic conductor with capacitive nature. This is because the phase shift angle ( $\theta$ ) is not constant at  $\theta = 90^\circ$ . The angle  $\theta$  values are found to vary and showing two peaks at the frequencies 458.9 Hz and 36.5 kHz, corresponding to  $\theta = 74.3^\circ$  and  $\theta = 69.2^\circ$ , respectively. In general, the values of  $\theta$  in this sample are large which are greater than  $40^\circ$ . This, by its role, indicated that the value of  $R_S$  and  $R_P$  are widely separated and is reflected in the values of the resistances obtained from the equivalent circuit and shown in table 1. Moreover, to have a Debye relaxation, the peak in  $\theta(f)$  should not equal to that of the complex impedance. This is confirmed in the present sample where we did not see a peak in the  $Z''(f)$  plot matches that of  $\theta(f)$  plot for the same sample. The phase shift angle is related to the energy dissipated as heat in the dielectric materials. As seen in fig 6.(a) the heat loss is expected to increase with frequency, but two peaks are observed signifying presence of more than a relaxation time. According to the model of Rezlescu, a peak appears when the frequency of the hopping of the charge carriers between two valence states of the same element matches with the frequency of the applied field. In SrLaFeTiO<sub>6</sub>, the valences states of Fe and Ti may exist as Fe<sup>3+</sup>/Fe<sup>2+</sup> and as Ti<sup>3+</sup>/Ti<sup>4+</sup> respectively. Thus, the peaks may be related to hopping between Fe<sup>2+</sup>  $\leftrightarrow$  Fe<sup>3+</sup> and Ti<sup>3+</sup>  $\leftrightarrow$  Ti<sup>4+</sup> ions pairs providing that there is an oxygen deficiency in the samples i.e. SrLaFeTiO<sub>6- $\delta$</sub> . Oxygen deficiency is reported by in SrLaMnTiO<sub>6- $\delta$</sub>  by D. Alonso et al using the thermal gravimetric analysis (TGA)[34].

**Table 1:** The fitting parameters which obtained using the equivalent circuits that shown in fig 7.

Constant Phase element	Parameters	SrLaFeTiO <sub>6</sub>	SrLaFe <sub>0.67</sub> Mn <sub>0.33</sub> TiO <sub>6</sub>	SrLaFe <sub>0.33</sub> Mn <sub>0.67</sub> TiO <sub>6</sub>	SrLaMnTiO <sub>6</sub>
Grain (R1+CPE1)	R1 (Ω)	3248.9	5390.1	8.99	37.024
	P1 x10 <sup>-9</sup>	10.16	0.61	-	-
	n1	0.95	0.94	-	-
	C1 (nF)	5.90	0.27	-	-
	τ 1(Sec)	19.17x10 <sup>-6</sup>	14.55x10 <sup>-7</sup>	-	-
Grain boundary (R2+CPE2)	R2 (Ω)	1.22x10 <sup>6</sup>	43055	125.7	-
	P2 x10 <sup>-9</sup>	9.45	17.45	1.10	-
	n2	0.92	0.81	0.92	-
	C2 (nF)	6.41	3.23	0.25	-
	τ 2(Sec)	7.82x10 <sup>-3</sup>	13.91x10 <sup>-5</sup>	31.43x10 <sup>-9</sup>	-
Electrode (R3+CPE3)	R3 (Ω)	95.68	26198	138.99	456.14
	P3 x10 <sup>-9</sup>	0.57	0.72	0.00019642	0.001
	n3	0.96	0.91	0.087	0.158
	C3 (nF)	0.28	0.25	0.006	190.93
	τ 3(Sec)	26.79x10 <sup>-9</sup>	65.50x10 <sup>-7</sup>	8.33x10 <sup>-10</sup>	87.09x10 <sup>-6</sup>
	Wsr2	1.87x10 <sup>5</sup>	2.0 x10 <sup>-14</sup>	2.0x10 <sup>-12</sup>	-
	Wsl	10.46	9.74	-	-
	C <sub>elec</sub> (nF)	-	-	1786.2	37.02
Electronic resistance	R <sub>e</sub> (Ω)	-	-	6.22	5.58

As mentioned above the inclusion of the Mn ions alters the conduction mechanism which should be reflected in the relaxation time of the conduction mechanism. The Cole-Cole plot of SrLaFe<sub>0.67</sub>Mn<sub>0.33</sub>TiO<sub>6</sub>, which shows two arcs, as well as the phase shift angle, depicted in fig 5.c and 6.b respectively. The complex shapes of the curves of the Cole-Cole plot and the  $\theta$  as a function of frequency indicate that there are two different relaxation processes for the bulk and grain boundary start separating. The arc lies on the higher frequency usually corresponds to the grain effects. These data are fitted to the model which is shown in fig 7.a. The values of the fitting parameters are given in table 1. In comparison to the parameters of SrLaFeTiO<sub>6-δ</sub>, the resistance of the grain boundary is reduced by a factor of two orders of magnitudes while the resistance

of the grain is increased slightly. Further, the relaxation time for both the grain and the grain size effects are reduced where they are moving from the hopping polarization domain to the dipolar polarization domain.

The values of  $\theta$ , see fig 5.c are seen to vary from small values up to around  $84^\circ$  i.e. the heat loss in SrLaFe<sub>0.67</sub>Mn<sub>0.33</sub>TiO<sub>6</sub> is increasing with frequency in a different manner as compared to SrLaFeTiO<sub>6- $\delta$</sub> . The peaks observed in  $\theta(f)$  of SrLaFeTiO<sub>6- $\delta$</sub>  are found to smear out. Thus, the Debye relaxation is weakened in the frequency range 20Hz-1MHz of the present measurements.

For the SrLaFe<sub>0.33</sub>Mn<sub>0.67</sub>TiO<sub>6</sub> the situations of the  $Z'$ - $Z''$  and  $\theta(f)$  plots, as seen in fig 5.c and in fig 6.c, are different. Low values of  $Z'$  and  $Z''$  are observed while the values of  $\theta(f)$  are found to be small and increase with frequency. In SrLaFe<sub>0.33</sub>Mn<sub>0.67</sub>TiO<sub>6</sub> the peak at low frequency for  $\theta(f)$  is disappeared and only one peak has appeared around 250 kHz which is not matching the frequency of the peak of the  $Z''(f)$  plot that falls around 440 kHz. Hence, the Debye relaxation is still present.

Attempts to analyze the data using the same equivalent circuit shown in fig 7.b are failed where the result of the fitting is not satisfactory and then the model needs to be modified. The data are then modeled using the equivalent circuit given in fig 7.b. Here, the contribution from the electronic conduction as expressed by the resistor  $R_e$  connected in parallel to the R-CPE's loops is included. The inclusion of the electronic contribution is inferred from the low values of  $Z'$  and  $Z''$ , and the value of  $\tau = 10^{-10}$  Sec which is comparable to that of the electronic polarization. The results of the fitting parameters are given in table 1. It can be observed in table 1, the relaxation time of the grain boundary

effect continues to decrease and becomes within the neighboring limits of the dipolar and atomic polarization domain.

The  $Z^{\prime} - Z^{\prime\prime}$  and  $\theta(f)$  plots of SrLaMnTiO<sub>6-δ</sub> are shown in fig 5.d and in fig 6.d respectively. The values of  $Z^{\prime}$  and  $Z^{\prime\prime}$  are the lowest in the series of the studied samples. In fig 6.d, the  $\theta(f)$  is found to increase without showing any peak within the frequency range of the measurement, but a peak is observed at a frequency around 750 kHz in the  $Z^{\prime\prime}(f)$  plot. Thus the Debye relaxation does not disappear in this range. The data are fitted to the equivalent circuit shown in fig 7.c. It must be noted here, that the best fitting is achieved without the inclusion of the CPE1 and the Warburg elements.

The effect of replacing the Fe ion in SrLaFeTiO<sub>6-δ</sub> by the Mn ions is found to alter the dielectric behavior of the samples. As noted in the frequency dependence of the real and the imaginary parts of the impedance of the samples, the values of the resistance are found to decrease with Mn-doping. This signifies that the mechanism of the transport process is changing. At the room temperature, the conduction is transforming from insulating in SrLaFeTiO<sub>6-δ</sub> to semiconducting or metallic in SrLaMnTiO<sub>6-δ</sub>. Therefore, and as a complementary tool for our present investigations, the temperature dependence of the electrical resistance of SrLaFeTiO<sub>6-δ</sub> and SrLaMnTiO<sub>6-δ</sub> are measured and shown in fig. 8. The electrical resistance of SrLaFeTiO<sub>6-δ</sub> is rapidly increasing below 100 K indicating the typical behavior of the insulating materials. While that of SrLaMnTiO<sub>6-δ</sub> shows a semiconductor-metal transition at around 250K. This transition is reported by I. Alvarez et al[12] to be 210K. The difference in the values of  $T_C$  may be related to the difference in the oxygen

content in both samples where the sample of I. Alvarez et al is prepared by a chemical method. This enhanced in conductivity may be explained by the  $Mn^{2+} \leftrightarrow Mn^{3+}$  pairs exist to switch on the double exchange mechanism that usually leads to a ferromagnetic metallic behavior [35]. Hence, this dc electrical measurement supports the claim that the present samples are in the intermediate doping of Mn may have mixed ionic-electronic conduction.

Generally speaking, the relaxation phenomena are associated with polarization where at low frequency the dipoles tend to align themselves along the direction of the electric field. At high frequencies the response of the dipoles to the rapid field is slow; hence their contribution to the polarization becomes negligible which leads to decrease of the real impedance with the increasing frequency[36]. In the lattice of the present double perovskites samples, the conduction mechanism could be related to the electron hopping between two adjacent octahedral sites and charge transfer might take place between  $Ti^{3+} \leftrightarrow Ti^{4+}$ ,  $Fe^{2+} \leftrightarrow Fe^{3+}$  and  $Mn^{2+} \leftrightarrow Mn^{3+}$  pairs. Generally, besides hopping, there is the polarization effect that plays a role(s) in the conductivity response to the frequency of double perovskites [37] where the applied electric field is known to displace the hopping electrons along with its direction to a certain value of the frequency. For the samples with low Mn concentration, the conduction may be understood if the polarization effect and the motion of space charge due to the inhomogeneous dielectric structure are considered[38]. With alternation of the direction of the electric field, the space charge carriers will also reverse their direction. At higher frequencies the time required for the reversal of the charge space carriers will be insufficient, hence lags behind the reversal of the applied field. With further increase in frequency, the space charge carriers will move

before the field reverses and makes virtually no contribution to the polarization of ionic double perovskites, hence the dielectric impedance of material decreases dramatically. For the samples with high Mn concentration, the conduction is governed by the double exchange mechanism where low resistance values and metallic behavior are observed at low temperature in SrLaMnTiO<sub>6-δ</sub>.

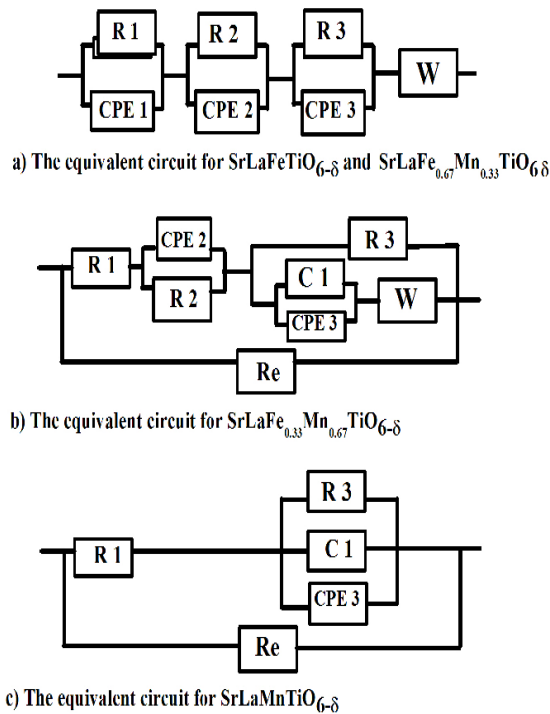


Fig 7: The equivalent circuits models used for fitting the impedance with the equiv

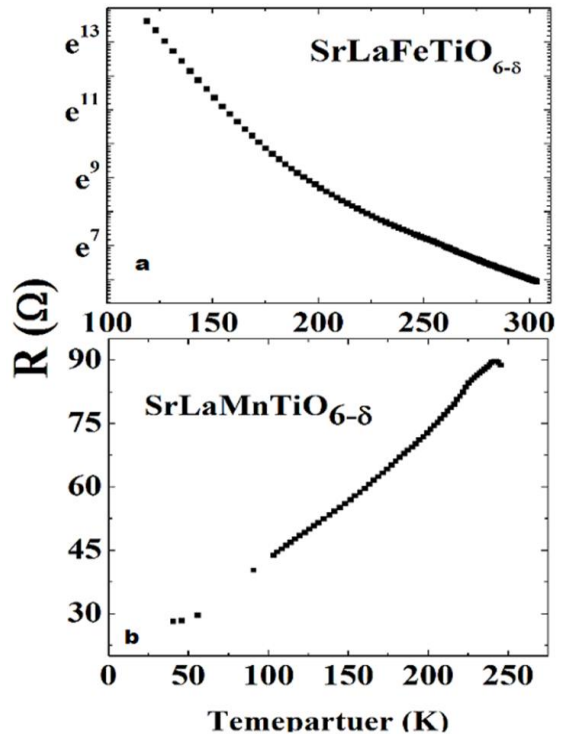


Fig 8: The DC-resistance measured as a function of temperature for SrLaFeTiO<sub>6-δ</sub> and SrLaMnTiO<sub>6-δ</sub>.

#### 4. Conclusions

The structural and the electrical properties of the double perovskite compounds SrLaFe<sub>1-x</sub>MnxTiO<sub>6-δ</sub>, (x= 0, 0.33, 0.67 & 1.0) have been studied by means of X-ray diffraction (XRD), the dielectric impedance measurements and supported by dc- resistivity measurement. The phase purity and the crystal structures of these compounds have been determined and confirmed by means of the standard Rietveld refinement method using the FullProf suite. The best fitting results showed that SrLaFeTiO<sub>6-δ</sub> is orthorhombic with space group Pnma, SrLaFe<sub>0.67</sub>Mn<sub>0.33</sub>TiO<sub>6-δ</sub> and SrLaFe<sub>0.33</sub>Mn<sub>0.67</sub>TiO<sub>6-δ</sub> have a cubic structure with space group Fm3m while SrLaMnTiO<sub>6-δ</sub> is tetragonal with space group I4/m. The charge density maps obtained from these structures have indicated that these compounds may have mixed ionic-electronic conduction. The dielectric impedance measurements in the range from 20 Hz to 1MHz and their analysis showed that there are more than one relaxation mechanisms. The data are found to follow the Debye relaxation type. A decrease in the resistance is noted when the Mn ions are introduced in the samples. The fall in the values of the electrical resistance is related to the possible occurrence of the double exchange mechanism among the Mn ions. This double exchange mechanism would take place providing that there is oxygen deficiency in the samples. The occurrence of the mixed ionic-electronic conduction and oxygen deficiency in these compounds qualify them to be used as gas sensors and/or solid oxide fuel cells (SOFC) materials. The dielectric impedance of SrLaFe<sub>0.67</sub>Mn<sub>0.33</sub>TiO<sub>6-δ</sub> is similar to (La,Sr)(Co,Fe)O<sub>3-δ</sub> the MIEC model.

#### References

1. Liu, Q., X. Dong, G. Xiao, F. Zhao, and F. Chens. *A novel electrode material for symmetrical SOFCs*. *Advanced Materials*, **22**, (48), 5478-5482, 2010.
2. Damo, U., M. Ferrari, A. Turan, and A. Massardos. *Solid oxide fuel cell hybrid system: a detailed review of an environmentally clean and efficient source of energy*. Energy, 2018.
3. Lu, Y., Y. Cai, L. Souamy, X. Song, L. Zhang, and J. Wangs. *Solid oxide fuel cell technology for sustainable development in China: An over-view*. *International Journal of Hydrogen Energy*, 2018.
4. Wang, Y., Z. Zhang, L. Zhang, Z. Luo, J. Shen, H. Lin, J. Long, J.C. Wu, X. Fu, and X. Wangs. *Visible-Light Driven Overall Conversion of CO<sub>2</sub> and H<sub>2</sub>O to CH<sub>4</sub> and O<sub>2</sub> on 3D-SiC@ 2D-MoS<sub>2</sub> Heterostructure*. *Journal of the American Chemical Society*, **140**, (44), 14595-14598, 2018.
5. Hossain, S., A.M. Abdalla, S.N.B. Jamain, J.H. Zaini, and A.K. Azads. *A review on proton conducting electrolytes for clean energy and intermediate temperature-solid oxide fuel cells*. *Renewable and Sustainable Energy Reviews*, **79**, 750-764, 2017.
6. Kharton, V.V., J.C. Waerenborgh, A.P. Viskup, S.O. Yakovlev, M.V. Patrakeev, P. Gaczyński, I.P. Marozau, A.A. Yaremchenko, A.L. Shaula, and V.V. Samakhval. *Mixed conductivity and Mössbauer spectra of (La<sub>0.5</sub>Sr<sub>0.5</sub>)<sub>1-x</sub>Fe<sub>1-y</sub>Al<sub>y</sub>O<sub>3-δ</sub> (x= 0–0.05, y= 0–0.30)*. *Journal of Solid State Chemistry*, **179**, (4), 1273-1284, 2006.
7. Kim, C.S., S.R. Bishop, and H.L. Tullers. *Electro-chemo-mechanical studies of perovskite-structured mixed ionic-electronic conducting SrSn<sub>1-x</sub>Fe<sub>x</sub>O<sub>3-x/2+δ</sub> part II: Electrical conductivity and cathode performance*. *Journal of Electroceramics*, **40**, (1), 57-64, 2018.
8. Tsipis, E., E. Kiselev, V. Kolotygin, J. Waerenborgh, V. Cherepanov, and V. Khartons. *Mixed conductivity, Mössbauer spectra and thermal expansion of (La, Sr)(Fe, Ni) O<sub>3-δ</sub> perovskites*. *Solid State Ionics*, **179**, (38), 2170-2180, 2008.
9. Jia, H., W. Zhou, S. Duan, H. Nan, F. Luo, and D. Zhus. *DC conductivity and AC impedance of Mn doped magnesia alumina spinel (MgAl<sub>2-2x</sub>Mn<sub>2x</sub>O<sub>4</sub>) over a large temperature range*. *Journal of the European Ceramic Society*, 2018.
10. Satapathy, A. and E. Sinhas. *A comparative proton conductivity study on Yb-doped BaZrO<sub>3</sub> perovskite at intermediate temperatures under wet N<sub>2</sub> environment*. *Journal of Alloys and Compounds*, **772**, 675-682, 2019.
11. Jasinski, P., V. Petrovsky, T. Suzuki, and H.U. Andersons. *Impedance studies of diffusion phenomena and ionic and electronic conductivity of cerium oxide*. *Journal of The Electrochemical Society*, **152**, (4), J27-J32, 2005.
12. Bashir, J. and R. Shaheens. *Structural and complex AC impedance spectroscopic studies of A<sub>2</sub>CoNbO<sub>6</sub> (A= Sr, Ba) ordered double perovskites*. *Solid State Sciences*, **13**, (5), 993-999, 2011.

13. Lai, W. and S.M. Hailes. *Impedance spectroscopy as a tool for chemical and electrochemical analysis of mixed conductors: a case study of ceria*. Journal of the American Ceramic Society, **88**, (11), 2979-2997, 2005.
14. Xia, T., X. Liu, Q. Li, J. Meng, and X. Caos. *Synthesis, structural and electrical characterizations of Sr<sub>2</sub>Fe<sub>1-x</sub>MxNbO<sub>6</sub> (M= Zn and Cu) with double perovskite structure*. Journal of alloys and compounds, **422**, (1-2), 264-272, 2006.
15. Marrero-López, D., J. Peña-Martínez, J. Ruiz-Morales, M. Martín-Sedeño, and P. Núñezs. *High temperature phase transition in SOFC anodes based on Sr<sub>2</sub>MgMoO<sub>6-δ</sub>*. Journal of Solid State Chemistry, **182**, (5), 1027-1034, 2009.
16. Zhang, L., Q. Zhou, Q. He, and T. Hes. *Double-perovskites A<sub>2</sub>FeMoO<sub>6-δ</sub> (A= Ca, Sr, Ba) as anodes for solid oxide fuel cells*. Journal of Power Sources, **195**, (19), 6356-6366, 2010.
17. Yang, E.-h., Y.-s. Noh, S. Ramesh, S.S. Lim, and D.J. Moons. *The effect of promoters in LaO. 9MO. 1NiO. 5FeO. 5O3 (M= Sr, Ca) perovskite catalysts on dry reforming of methane*. Fuel Processing Technology, **134**, 404-413, 2015.
18. Teixeira, A.R.F.A., A. de Meireles Neris, E. Longo, J.R. de Carvalho Filho, A. Hakki, D. Macphee, and I.M.G. dos Santoss. *SrSnO<sub>3</sub> perovskite obtained by the modified Pechini method—Insights about its photocatalytic activity*. Journal of Photochemistry and Photobiology A: Chemistry, **369**, 181-188, 2019.
19. El Hachmi, A., Y. Tamraoui, B. Manoun, R. Haloui, M. Elaamrani, I. Saadoune, L. Bih, and P. Lazors. *Synthesis and Rietveld refinements of new ceramics Sr<sub>2</sub>CaFe<sub>2</sub>WO<sub>9</sub> and Sr<sub>2</sub>PbFe<sub>2</sub>TeO<sub>9</sub> perovskites*. Powder Diffraction, **33**, (2), 134-140, 2018.
20. Correia, V., K. Mitra, H. Castro, J. Rocha, E. Sowade, R. Baumann, and S. Lanceros-Mendezs. *Design and fabrication of multilayer inkjet-printed passive components for printed electronics circuit*
21. John, R.A., P.P. Boix, C. Yi, C. Shi, M. Scott, S.A. Veldhuis, A.M. Minor, S.M. Zakeeruddin, L.H. Wong, and M. Grätzels. *Atomically Altered Hematite for Highly Efficient Perovskite Tandem Water-Splitting Devices*. ChemSusChem, **10**, (11), 2449-2456, 2017.
22. Kleinlogel, C. and L. Gaucklers. *Mixed electronic-ionic conductivity of cobalt doped cerium gadolinium oxide*. Journal of electroceramics, **5**, (3), 231-243, 2000.
23. Burnat, D., G. Nasdaurk, L. Holzer, M. Kopecki, and A. Heels. *Lanthanum doped strontium titanate-ceria anodes: deconvolution of impedance spectra and relationship with composition and microstructure*. Journal of Power Sources, **385**, 62-75, 2018.
24. Lunkenheimer, P., T. Götzfried, R. Fichtl, S. Weber, T. Rudolf, A. Loidl, A. Reller, and S. Ebbinghaus. *Apparent giant dielectric constants, dielectric relaxation, and ac-conductivity of hexagonal perovskites La<sub>1-2</sub>Sr<sub>2-7</sub>BO<sub>7-33</sub> (B= Ru, Ir)*. Journal of Solid State Chemistry, **179**, (12), 3965-3973, 2006.

25. Ruiz-Morales, J.C., D. Marrero-López, J.T. Irvine, and P. Núñezs. *A new alternative representation of impedance data using the derivative of the tangent of the phase angle: Application to the YSZ system and composites*. Materials research bulletin, **39**, (9), 1299-1318, 2004.
26. Nadeem, M., M.J. Akhtar, and A.Y. Khans. *Effects of low frequency near metal-insulator transition temperatures on polycrystalline La<sub>0.65</sub>Ca<sub>0.35</sub>Mn<sub>1-y</sub>FeyO<sub>3</sub> (where y=0.05–0.10) ceramic oxides*. Solid State Communications, **134**, (6), 431-436, 2005.
27. Kumar, M.M., A. Srinivas, and S. Suryanarayan. *Structure property relations in BiFeO<sub>3</sub>/BaTiO<sub>3</sub> solid solutions*. Journal of Applied Physics, **87**, (2), 855-862, 2000.
28. Maity, S.K., A. Dutta, S. Kumar, and T. Sinhas. *Electrical properties of Ba<sub>2</sub>YbNbO<sub>6</sub>: an impedance spectroscopy study*. Physica Scripta, **88**, (6), 065702, 2013.
29. Reddy, Y.S., Y. Markandeya, B.A. Rao, and G. Bhikshamaiahs. *Characterization and impedance study of Ba<sub>2</sub>CeZrO<sub>6</sub> double perovskite*. Journal of Materials Science: Materials in Electronics, **29**, (4), 2966-2973, 2018.
30. Jamnik, J. and J. Maier. *Generalised equivalent circuits for mass and charge transport: chemical capacitance and its implications*. Physical Chemistry Chemical Physics, **3**, (9), 1668-1678, 2001.
31. Honea, J.W.s. *Dynamic Modeling of Electrochemical Cells With Application to Proximal Three-Terminal Electrolysis*. Journal, (Issue), 2011.
32. Leshem, A., E. Gonen, and I. Riess. *Nonlinear I–V relations and hysteresis in solid state devices based on oxide mixed-ionic–electronic conductors*. Nanotechnology, **22**, (25), 254024, 2011.
33. Yang, W., J. Lu, J. Weng, W. Jia, L. Ji, J. Xiao, Z. Shan, J. Liu, H. Tian, and Q. Jis. *Prevalence of diabetes among men and women in China*. New England Journal of Medicine, **362**, (12), 1090-1101, 2010.
34. Rezlescu, N. and E. Rezlescu. *Dielectric properties of copper containing ferrites*. physica status solidi (a), **23**, (2), 575-582, 1974.
35. Medvedkin, G.A., T. Ishibashi, T. Nishi, K. Hayata, Y. Hasegawa, and K. Satos. *Room temperature ferromagnetism in novel diluted magnetic semiconductor Cd<sub>1-x</sub>Mn<sub>x</sub>GeP<sub>2</sub>*. Japanese Journal of Applied Physics, **39**, (10A), L949, 2000.
36. Kao, K.C.s. *Dielectric phenomena in solids*. Journal, (Issue), 2004.
37. Maxwell, J.C.s. *Electricity and magnetism*. Journal, **2**, (Issue), 1954.
38. Gul, I. and A. Maqsoods. *Structural, magnetic and electrical properties of cobalt ferrites prepared by the sol–gel route*. Journal of Alloys and Compounds, **465**, (1-2), 227-231, 2008.

